phys. stat. sol. (a) 49, 169 (1978)

Subject classification: 16; 22.4.1

Institut für Angewandte Physik der Universität Karlsruhe

Photovoltage at the Metal–CdS Schottky Contact

By

R. BUTENDEICH and W. RUPPEL

In honour of Prof. Dr. F. STÖCKMANN's 60th birthday

Photovoltages at a metal–CdS Schottky contact occur at photon energies that are smaller than the CdS band gap. They may be due either to photoemission of electrons from the metal into the CdS or to hole generation in the CdS. The first mechanism is shown to occur in conducting CdS. From its observation values for the attenuation length of the photoexcited electrons in Au are derived as a function of photon energy. The second mechanism is shown to occur in insulating CdS. At intermediate conductivities of the CdS photoemission is found for small photon energies, while minority carrier generation in the CdS is responsible for the generation of a photo-e.m.f. at somewhat higher photon energies.

Photospannungen an einem Metall–CdS-Schottky-Kontakt entstehen bei Belichtung auch mit Photonen, deren Energie kleiner ist als der Bandabstand des CdS. Diese Photospannungen beruhen entweder auf Photoemission von Elektronen aus dem Metall in das CdS oder auf Löchererzeugung im CdS. Bei CdS hoher Leitfähigkeit tritt der erstgenannte Mechanismus auf. Aus seiner Beobachtung werden Werte für die Reichweite der optisch erzeugten Elektronen in Au als Funktion der Photonenenergie gewonnen. Der zweitgenannte Mechanismus tritt in isolierendem CdS auf. Im Zwischengebiet der Leitfähigkeit des CdS wird für kleine Photonenenergien Photoemission beobachtet, während die Erzeugung von Minoritätsträgern im CdS bei größeren Photonenenergien die Photospannung verursacht.

1. Introduction

The occurrence of a photoelectromotive force (photo-e.m.f. or photovoltage) at a metal–CdS Schottky contact is observed also for photons the energy of which is smaller than the CdS band gap [1]. The origin of this photo-e.m.f. has been explained in two different ways:

1. Excitation of the metal adjacent to the semiconductor and emission of electrons from the metal into the semiconductor [2 to 5]. This operation is analogous to the vacuum photocell.

2. Excitation in the semiconductor space charge layer and creation of mobile minority carriers [6 to 12].

Both excitation mechanisms have in common that the band gap energy does not present a low-energy limit for the photon energy at which a photo-e.m.f. is observed (Fig. 1). Electrons may be emitted from the metal when their excitation energy exceeds that of the Schottky potential barrier at the contact which may be considerably less than the band gap. Free minority carriers in the semiconductor may as well be created by photons of smaller energy than that of the band gap.

Conclusions about the concentration and the energetic distribution of traps and recombination centres from measurements of the photoconduction under applied voltage for majority carriers and from measurements of the photo-e.m.f. for minority carriers have been the aim of the work of Stöckmann and his coworkers in the last few years. It is evident that conclusions on the properties of minority carrier traps and recombination centres may only be drawn from measurements of the photo-e.m.f.

if it is asserted that the observed photovoltage is due to minority carrier generation in the semiconductor. On the other hand, detection of the photovoltage due to electron excitation in the contact metal may lead to the determination of properties of the excited metal electron gas.

It will be shown in the present paper that the parameter which delineates the occurrence of either of these mechanisms is the position of the Fermi level in the dark and hence the dark conductivity of the CdS. As we will see, for a low-lying Fermi level, namely insulating CdS, excitation of minority carriers prevails as the mechanism responsible for the photo-e.m.f., while for a shallow Fermi level, namely rather conducting CdS, it is electron emission from the metal into the CdS.

2. Origin of the Photovoltage

2.1 Photoemission into CdS

Electrons excited in the metal contact layer and crossing the metal–CdS boundary generate an e.m.f. if they penetrate into the CdS at least by the distance x_m (Fig. 1). x_m denotes the maximum of the potential. The distribution of the electrical potential in the CdS results from the superposition of a contribution from the difference in the electron chemical potential at the metal–semiconductor boundary and a contribution from the image force. The distance x_m from the metal–CdS boundary is [13]

$$x_m = 1.9 \times 10^{-4} \left(\frac{\varepsilon F_0}{\mathrm{V/cm}} \right)^{1/2} \mathrm{cm}\,, \tag{1}$$

where F_0 denotes the field strength at the boundary without consideration of the image force, and ε the dielectric constant.

Assuming an electron mean free path in the CdS in the order of 1 to 5 nm and considering that the hot electrons emitted from the metal may pass the barrier maximum

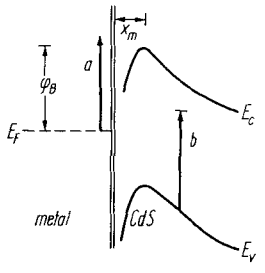

Fig. 1

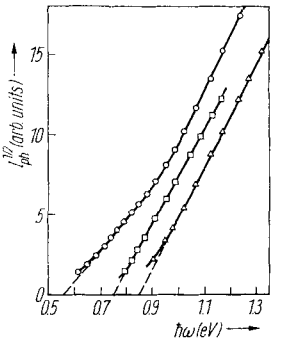

Fig. 2

Fig. 1. Metal–CdS Schottky contact with the contribution of the image force. E_F denotes the Fermi level, E_c and E_v the band edges of conduction and valence band. x_m is the distance of the potential maximum from the metal–CdS interface. φ_B is the barrier height. The transition a shows an excitation of the metal electron gas beyond φ_B. The transition b shows an excitation with equal photon energy as transition a leading to a mobile hole in the CdS

Fig. 2. Square root of the short-circuit photocurrent as a function of photon energy (Fowler plot) for various metal–CdS contacts. The extrapolation to the abscissa yields the barrier height φ_B. Dark conductivity of the CdS $\sigma = 10^{-1}\,(\Omega\,\mathrm{cm})^{-1}$. For the Au and Pt contact $T = 295$ K. For the Ag contact $T = 110$ K. ○ Ag–CdS, △ Pt–CdS, □ Au–CdS

at x_m only after several collisions with LO-phonons, one is to expect the generation of a photo-e.m.f. by photoemission into the CdS for values of x_m in the range

$$x_m \lessapprox 10 \text{ to } 50 \text{ nm} .$$

The boundary field strength F_0 of a Schottky electron depletion layer

$$F_0 = \left(\frac{2\sigma U_D}{\mu_n \varepsilon \varepsilon_0}\right)^{1/2} \tag{2}$$

yields in combination with (1) for values of the diffusion potential $U_D = 0.6$ V and the electron mobility $\mu_n = 10$ cm²/Vs a conductivity range for CdS of

$$\sigma \gtrsim 10^{-5} (\Omega \text{ cm})^{-1} \tag{3}$$

in which an e.m.f. due to photoemission of electrons from the metal into CdS should be observable.

Experimentally, Fig. 2 shows a Fowler plot for an illuminated CdS contact with Au, Ag, and Pt. The samples were prepared by evaporating the metal contact on to the CdS crystal while the crystal was cleaved in high vacuum under the metal vapour stream. The fact that the square root of the short-circuit photocurrent depends linearly on the photon energy of the incident photons above the current threshold, points to generation of the photocurrent by photoemission. The values for the potential barrier heights φ_B of the Schottky barrier, as derived from the threshold photon energies in Fig. 2, are in good agreement with observations reported in the literature. A review of φ_B of various material combinations is presented in [14]. Lepley and Ravelet find for Au on polycrystalline CdS films of 1 to 100 Ω cm that φ_B lies in the range 0.6 to 0.9 eV according to the treatment of the CdS surface before the Au deposition [15]. φ_B is related to the photo-e.m.f. and to the thickness of an insulating interface layer which stems either from chemisorbed impurities or oxide formation. The existence of

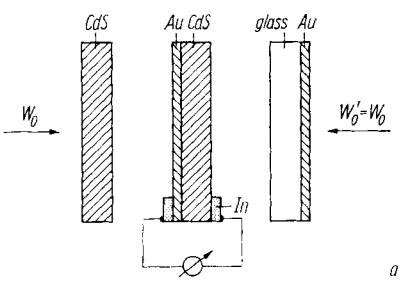

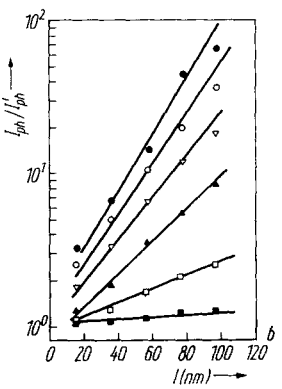

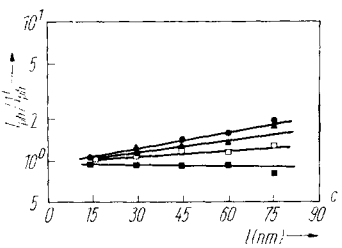

Fig. 3. a) Illumination of a Au–CdS contact from two sides with equal light intensities $W_0 = W_0'$. An additional CdS crystal and Au layer provide equal light intensities incident on the Au–CdS interface. b) Ratio I_{ph}/I'_{ph} of the short-circuit photocurrents measured with the arrangement shown in a) as a function of the Au-layer thickness l at different photon energies $\hbar\omega$ of monochromatic light of the intensity $W_0 = W_0'$ in a). Dark conductivity of the CdS crystal $\sigma = 10^{-1}$ $(\Omega \text{ cm})^{-1}$. ● $\hbar\omega = 1.13$, ○ 1.27, ▽ 1.44, ▲ 1.69, □ 1.92, ■ 2.27 eV. c) As b), but for a CdS crystal of the dark conductivity $\sigma = 10^{-12}$ $(\Omega \text{ cm})^{-1}$ (values of $\hbar\omega$ as under b))

chemically reacted interface layers has recently been demonstrated by the energy loss spectra of low-energy electrons [16]. Other observations on Au contacts on CdS single crystals or polycrystalline films yield also values in this range, namely $\varphi_B = (0.67 \pm 0.03)$ eV [17] and $\varphi_B = 0.7$ to 0.8 eV [18].

Values for Cu have not been included in Fig. 2. In agreement with Lepley et al. [19] who observe a change of the short-circuit photocurrent upon heat treatment for a Cu contact in contrast to a Au contact, we find a time variation of φ_B for Cu even without heat treatment in the course of several weeks. Photoemission, originally observed at the Cu–CdS contact, weakens and at the same time the characteristic features of a photo-e.m.f. as due to minority carrier generation in the CdS become more and more pronounced. Also, the resistivity of the CdS close to the Cu layer increases. These observations are accounted for by diffusion of Cu from the contact into the CdS. It appears that certain contradictory observations on the photovoltaic behaviour of Cu layers deposited on CdS may be readily reconciled if a different degree of diffusion of Cu into the CdS at different times after the Cu deposition is considered.

A direct proof for the contribution of photoemission to the generation of the e.m.f. at a metal–CdS contact for conducting CdS, and for an origin of the photo-e.m.f. different from photoemission for insulating CdS is constituted by the following experiment: The Au–CdS interface is illuminated from both sides in a completely symmetrical way (Fig. 3a). When illuminated from the Au side (left in Fig. 3a) through an additional CdS crystal, a short-circuit photocurrent I_{ph} results. If illuminated from the CdS side through an additional Au layer (right in Fig. 3a), a short-circuit photocurrent I'_{ph} is obtained. The number of photons arriving at the Au–CdS interface is the same for both illuminations. The observed ratio I_{ph}/I'_{ph} is shown in Fig. 3b and c as a function of the thickness l of the Au contact layer. It is seen that for CdS of high conductivity ($\sigma = 10^{-1}$ $(\Omega\,\mathrm{cm})^{-1}$) in Fig. 3b the ratio I_{ph}/I'_{ph} does not equal unity. Particularly for photons of high energy it strongly increases with increasing thickness l of the Au contact layer. An indicator for the optimum thickness of evaporated metal layers in Schottky barrier solar cells is described in [20]. For CdS of low conductivity ($\sigma = 10^{-12}$ $(\Omega\,\mathrm{cm})^{-1}$) the ratio I_{ph}/I'_{ph}, shown in Fig. 3c, is almost equal to unity independently of the incident photon energy and of the Au layer thickness.

The dependence of I_{ph}/I'_{ph} on l and on $\hbar\omega$ in Fig. 3b may readily be understood if the origin of both I_{ph} and I'_{ph} is taken into account as being due to photoemission. Let L denote the attenuation length or range of the optically excited electrons in the Au metal. Provided that for the penetration depth α^{-1} of the light into the layer holds that $\alpha^{-1} < l$ and $\alpha^{-1} < L$, the ratio I_{ph}/I'_{ph} is given by

$$\frac{I_{ph}(l, \hbar\omega)}{I'_{ph}(l, \hbar\omega)} = \exp\left[l\left(\alpha - \frac{1}{L}\right)\right]. \tag{4}$$

Evaluating the curves in Fig. 3b and considering $\alpha = \alpha(\hbar\omega)$ for Au as shown in Fig. 4, one finds for the attenuation length L of the photoexcited electrons in the Au

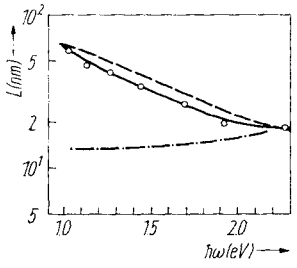

Fig. 4. Attenuation length of optically excited hot electrons in Au at $T = 295$ K as a function of excitation energy. The open circles are deduced from the measurements shown in Fig. 3b. For comparison, results of Sze et al. [21] (– – – –) are given. The dash-dotted line shows the penetration depth of light in Au

layer as a function of the excitation energy $\hbar\omega$ the values shown in Fig. 4. They are in close agreement with values obtained by Sze et al. [21] from measurements on the collection of photoexcited electrons across Schottky barriers in Au–GaP and Au–Si structures.

2.2 Minority carrier generation in the CdS

With decreasing σ of the CdS the distance x_m of the potential barrier maximum from the metal–CdS interface increases (Fig. 1). For large values of x_m photoemission of electrons from the metal cannot lead any more to the generation of a photo-e.m.f. This expectation is borne out by the results shown in Fig. 3c. The fact that for insulating CdS the photovoltage has the same value irrespective of the side from which the CdS–metal interface is illuminated, demonstrates that the excitation leading to the generation of the photo-e.m.f. may not be located in the metal but in the CdS adjacent to the interface. If the excitation takes places in the CdS, it must be the generation of mobile holes as the minority carriers in the CdS that leads to the observed photovoltage.

The generation of minority carriers in insulating CdS as the source of the photo-e.m.f. in a CdS–metal contact is demonstrated by its correlation with the quenching of the photocurrent under externally applied voltage [11]. Fig. 5 shows the spectral dependence of the photovoltage under two-photon-beam excitation (Fig. 5a) and the quenching of the photocurrent under applied voltage (Fig. 5b). In both cases one photon beam of 2.0 eV photons is incident on the Au–CdS contact of CdS with a dark conductivity $\sigma = 10^{-12}\,(\Omega\,\mathrm{cm})^{-1}$. The abscissa in Fig. 5 shows the photon energy of the second photon beam. The maxima of the photovoltage are seen to coincide in photon energy with the minima of the photocurrent under applied voltage. They occur at photon energies following from a model by Hemila and Bube [22]. The quenching of the photocurrent under applied voltage by additional illumination with photons of lower energy is well known to be due to the excitation of minority carriers. This exci-

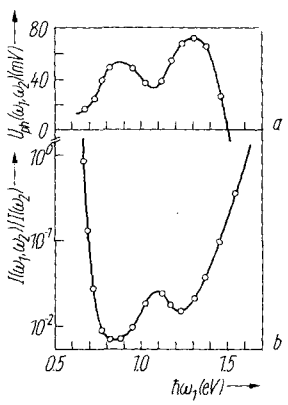

Fig. 5

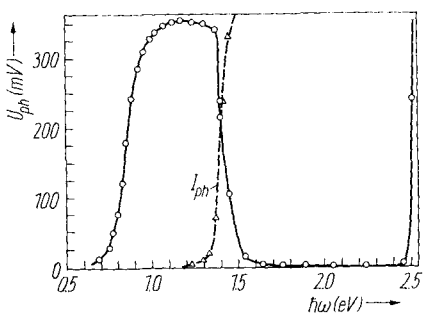

Fig. 6

Fig. 5. a) Photovoltage U_{ph} at Au–CdS contact under two-beam illumination as a function of the photon energy of the second beam. The photon energy of the first beam is 2.0 eV. Dark conductivity of the CdS crystal $\sigma = 10^{-12}\,(\Omega\,\mathrm{cm})^{-1}$. b) Photocurrent under externally applied voltage for the same illumination and the same sample as a). The quenching extrema occur at the same photon energies as the maxima of the photovoltage

Fig. 6. Photovoltage U_{ph} and short-circuit photocurrent I_{ph} (dashed line) of a Au–CdS contact at $T = 110$ K as a function of photon energy. Dark conductivity of the CdS crystal $\sigma = 10^{-9}\,(\Omega\,\mathrm{cm})^{-1}$

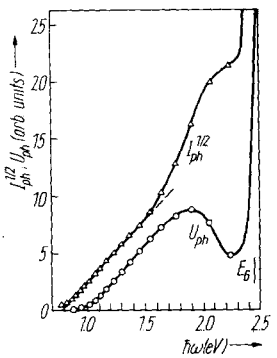

Fig. 7. Photovoltage U_{ph} and square root of the short-circuit photocurrent $I_{ph}^{1/2}$ (Fowler plot) of a Au–CdS contact at $T = 295$ K. Dark conductivity of the CdS crystal $\sigma = 10^{-5}$ $(\Omega\ \mathrm{cm})^{-1}$

tation causes an enhanced recombination of majority carriers and hence a reduction of the photocurrent.

On the other hand, the holes as minority carriers can be quenched as well by the generation of electrons as the majority carriers. An example for this effect is shown in Fig. 6. At a Au–CdS contact at 110 K with CdS of a dark conductivity of 10^{-9} $(\Omega\ \mathrm{cm})^{-1}$ a maximum of the photovoltage is observed at about half the band-gap value due to minority carrier generation in the CdS by two-step excitation of electrons from the valence band into the conduction band. For the photovoltage at still lower photon energies a small contribution of photoemission from the Au contact may not be excluded. Around 1.4 eV, however, a strong generation of electrons is indicated by a steep rise of the short-circuit photocurrent due to a reduction of the series resistance of the CdS. As Fig. 6 shows, the rise of the short-circuit photocurrent is accompanied by a pronounced decrease of the photovoltage over the spectral region up to the CdS band gap. This decrease of the photo-e.m.f. is due to the quenching of the holes by photo-excited electrons.

In a Au–CdS contact with CdS of an intermediate value of the conductivity, both mechanisms for the generation of a photo-e.m.f., photo emission from the Au layer and hole generation in the CdS, may be observed. This is shown in Fig. 7 for CdS of a dark conductivity $\sigma = 10^{-5}$ $(\Omega\ \mathrm{cm})^{-1}$. At small photon energies photoemission is observed in agreement with Fig. 2. With increasing photon energies the short-circuit photocurrent increases somewhat more strongly than expected from a Fowler plot. This effect could be due to a reduction of the series resistance in the CdS and is not necessarily incompatible with predominant electron emission from the Au layer as the source of U_{ph} and I_{ph} in Fig. 6. With further increase of the incident photon energy the photovoltage is, however, observed to decrease. This behaviour cannot be accounted for by photoemission but points to hole generation in the CdS as the predominant source of the photo-e.m.f.

3. Conclusions

In conclusion, it may be stated that the mechanism of the generation of a photo-e.m.f. at photon energies smaller than the band gap in a metal–CdS Schottky contact depends on the conductivity of the CdS. For CdS with a dark conductivity $\sigma > 10^{-5}$ $(\Omega\ \mathrm{cm})^{-1}$, the photo-e.m.f. is almost entirely due to the emission of photo-excited electrons from the metal into the CdS in close analogy to the emission of electrons from the metal into vacuum in a vacuum photocell. Into CdS with a dark conductivity $\sigma < 10^{-9}$ $(\Omega\ \mathrm{cm})^{-1}$ no photoemission of electrons occurs beyond the potential maximum in the CdS. The observed photo-e.m.f. is due to the optical generation of mobile holes as the minority carriers in CdS. In metal–CdS contacts with conductivity

values between the extremes of the conducting and the insulating type both mechanisms may occur. While at the tail of small photon energies the photo-e.m.f. is predominantly due to photo emission, at higher photon energies, but still at values below that of the CdS band gap, hole generation in the CdS is observed to be the prevailing mechanism for the generation of a photo-e.m.f.

References

[1] D. C. Reynolds, G. Leies, L. L. Antes, and R. E. Marburger, Phys. Rev. **96**, 533 (1954).
[2] R. Williams and R. H. Bube, J. appl. Phys. **31**, 968 (1959).
[3] C. A. Mead and W. G. Spitzer, J. appl. Phys. **34**, 3061 (1963).
[4] C. A. Mead, Solid State Electronics **9**, 1023 (1966).
[5] A. M. Goodman, J. appl. Phys. **35**, 573 (1964).
[6] H. G. Grimmeiss and R. Memming, J. appl. Phys. **33**, 2217 (1961).
[7] E. D. Fabricius, J. appl. Phys. **33**, 1597 (1962).
[8] J. Woods and I. A. Champion, J. Electronics **7**, 243 (1959).
[9] N. Duc Cuong and J. Blair, J. appl. Phys. **37**, 1660 (1966).
[10] P. N. Keating, J. Phys. Chem. Solids **24**, 1101 (1963).
[11] W. Palz and W. Ruppel, phys. stat. sol. **15**, 649 (1966).
[12] S. Yu. Pavelets and G. A. Fedorus, Ukr. fiz. Zh. **14**, 620 (1969).
[13] R. Williams, in: Semiconductors and Semimetals, Vol. 6, Academic Press, New York/London 1970.
[14] J. O. McCaldin, T. C. McGill, and C. A. Mead, J. Vacuum Sci. Technol. **13**, 802 (1976).
[15] B. Lepley and S. Ravelet, phys. stat. sol. (a) **33**, 517 (1976).
[16] L. J. Brillson, Phys. Rev. Letters **40**, 260 (1978).
[17] G. Lubberts, J. appl. Phys. **47**, 365 (1976).
[18] V. M. Marakhonov, V. M. Busov, E. L. Seisyan, and M. M. Shulinskaya, Zh. tekh. Fiz., Pisma **2**, 356 (1976).
[19] B. Lepley, S. Ravelet, and P. Renard, phys. stat. sol. (a) **22**, K191 (1974).
[20] Juh Tzeng Lue, J. Phys. E **11**, 84 (1978).
[21] S. M. Sze, I. L. Moll, and T. Sugano, Solid State Electronics **7**, 509 (1964).
[22] S. O. Hemila and R. H. Bube, J. appl. Phys. **38**, 5258 (1967).

(Received June 23, 1978)